Available online at www.sciencedirect.com

ScienceDirect

IFAC Papers Online CONFERENCE PAPER ARCHIVE

IFAC PapersOnLine 52-30 (2019) 155–160

Autonomous Travel of Lettuce Harvester using Model Predictive Control

T. Mitsuhashi * **Y. Chida** ** **M. Tanemura** ***

* *Graduate School of Science and Technology, Shinshu University, Nagano, Japan, (e-mail: 19w4058e@shinshu-u.ac.jp).*
** *Faculty of Engineering, Shinshu University, Nagano, Japan, (e-mail: chida@shinshu-u.ac.jp)*
*** *Faculty of Engineering, Shinshu University, Nagano, Japan, (e-mail: tanemura@shinshu-u.ac.jp)*

Abstract: Autonomous travel of agricultural machines/robots is achieved by movement along a straight line based on a map with the global positioning system (GPS). However, when farm produce such as lettuce is not grown in a straight line, the robots equipped with GPS might damage the lettuce intended for harvesting. With regard to this problem, autonomous travel using local information can improve harvesting accuracy. In this paper, we propose an autonomous travel method for a lettuce harvester with on-off actuators based on the relative positions of the lettuce and the harvest machine obtained via a camera. This study adopts model predictive control (MPC) to ensure that the vehicle follows the positions of some lettuce located ahead in the same line if the vehicle includes the restriction of turning radius. To facilitate the application of an optimal method for determining an optimal input sequence in MPC, we transform a kinematics model of the vehicle into the time-state control form. The effectiveness of the proposed method is shown through numerical examples.

Keywords: Autonomous vehicles, Harvester, Tracked vehicle, On-off actuators, Model predictive control, Nonlinear models, Time-state Control Form

1. INTRODUCTION

The population of farmers is reducing in Japan. Therefore, autonomous travel robots are being increasingly used in agriculture (Iida et al. (2013)). Many autonomous travel robots usually move in a straight line based on a map with the global positioning system (GPS) (Iida et al. (2013); Noguchi et al. (2004); O'Connor et al. (1996)). In contrast, in the case of vegetables, even if they are planted in a straight line, they usually grow off-center and rarely grow in a straight line. Therefore, it is required to automatically harvest with the same quality as manual procedures in the Japan crop market. Therefore, control of an automatic harvester that can deal with several centimeters accuracy of the harvest target is required. GPS cannot recognize the variation in the positions of the farm produce. A control method based on the relative positions of the farm produce and the harvest machine can overcome this problem. Kise et al. (2005) detected a ridge of farm produce as a straight line using a camera installed on a harvest machine. Then, the harvest machine follows a straight line. However, the machine cannot detect each item of the produce, and therefore, does not harvest all items accurately. Studies on tracked vehicle control have devised methods with continuous inputs (Keicher and Seufert (2000); Fukao et al. (2000); Nagasaka et al. (2004); Ahmadi et al. (2000)). In contrast, methods using on-off actuators have been scarcely studied because of theoretical difficulties. However, on-off actuators are superior with respect to maintenance and cost compared with continuous input actuators.

Motivated by these aspects, we propose an autonomous travel method for a lettuce harvester with on-off actuators based on the relative positions of the lettuce and the harvest machine obtained via a camera. This study adopts model predictive control (MPC) to ensure that the vehicle follows not only the position of the nearest lettuce but also the positions of some lettuce located ahead in the same line in the condition that the vehicle includes the restriction of turning radius. To facilitate the application of the optimal method (Maruyama et al. (2013)) for determining an optimal input sequence in MPC, we transform a kinematics model of the vehicle into the time-state control form (Sampei (1994); Sampei et al. (1996)). The effectiveness of the proposed method is verified through numerical examples.

2. PROBLEM FORMULATION

2.1 Systems

We consider the tracked vehicle with on-off actuators for a lettuce harvester such as the one seen in Fig. 1. This section discusses a kinematics model of the tracked vehicle shown in Fig. 2. It is assumed that the tracked vehicle does not slip. Then, the velocity v of the center of the vehicle, tangential velocity ω, and turning radius ρ are given by

⋆ Some part of this work was supported by JSPS KAKENHI Grant Number JP17K18876.

10.1016/j.ifacol.2019.12.514

$$v(t) = \frac{v_l(t) + v_r(t)}{2}, \tag{1}$$

$$\omega(t) = \frac{-v_l(t) + v_r(t)}{D_t}, \tag{2}$$

$$\rho(t) = \frac{D_t(v_l(t) + v_r(t))}{2(-v_l(t) + v_r(t))}, \quad (v_l(t) \neq v_r(t)), \tag{3}$$

where v_l and v_r are the velocities of left-/right-hand side crawlers, respectively, D_t is the distance between the left-hand and right-hand side crawlers, and D_h is the distance between the center of the vehicle and the top of the harvest unit. When the velocities are $v_l(t) = v_r(t)$, the turning radius ρ becomes infinity. Therefore, (3) is defined for $v_l(t) \neq v_r(t)$, and if $v_l(t) = v_r(t)$, the turning radius is defined as infinity in this study. For Eqs. (1)-(3), in the global coordinates, the kinematics model of the tracked vehicle with the continuous input is described as

$$\frac{dx}{dt}(t) = -v(t)\sin\theta(t), \tag{4}$$

$$\frac{dy}{dt}(t) = v(t)\cos\theta(t), \tag{5}$$

$$\frac{d\theta}{dt}(t) = \omega(t), \tag{6}$$

where $\mathrm{P}(x, y)$ are the coordinates of the center of the vehicle, and θ is the angle between the center line of the vehicle and the y-axis. Then, $v = u_1$ and $\omega = u_2$ are regarded as control inputs, and the kinematics model is described as the non-linear system

$$\dot{\boldsymbol{x}}(t) = \boldsymbol{f_1}(\boldsymbol{x}(t))u_1(t) + \boldsymbol{f_2}u_2(t), \tag{7}$$

$$\boldsymbol{x}(t) := \begin{bmatrix} x(t) \\ y(t) \\ \theta(t) \end{bmatrix}, \ \boldsymbol{f_1}(\boldsymbol{x}(t)) := \begin{bmatrix} -\sin\theta(t) \\ \cos\theta(t) \\ 0 \end{bmatrix}, \ \boldsymbol{f_2} := \begin{bmatrix} 0 \\ 0 \\ 1 \end{bmatrix}.$$

The Lie bracket of (7) is given by

$$[\boldsymbol{f_1}, \boldsymbol{f_2}](\boldsymbol{x}) = \frac{\partial \boldsymbol{f_2}}{\partial \boldsymbol{x}}\boldsymbol{f_1}(\boldsymbol{x}) - \frac{\partial \boldsymbol{f_1}}{\partial \boldsymbol{x}}\boldsymbol{f_2}(\boldsymbol{x}) = \begin{bmatrix} \cos\theta(t) \\ \sin\theta(t) \\ 0 \end{bmatrix}. \tag{8}$$

The three-dimensional space is spanned by (8), $\boldsymbol{f_1}(\boldsymbol{x})$, and $\boldsymbol{f_2}(\boldsymbol{x})$. Therefore, (7) is globally controllable from Chow's theorem (William (1995)).

In this study, the tracked vehicle is driven with on-off actuators, and the velocities v_l and v_r are defined as the binary inputs as follows:

$$v_l, v_r \in \{0, v_{on}\}.$$

In addition, it is assumed that control inputs $v_l = 0$ and $v_r = 0$ are not chosen simultaneously. This assumption means that the vehicle does not stop. Using this assumption, control inputs (u_1, u_2) are defined as

$$(u_1, u_2) \in \{(u_{1l}, u_{2l}),\ (u_{1s}, 0),\ (u_{1r}, u_{2r})\}, \tag{9}$$

where

$$u_{1l} = \frac{0 + v_{on}}{2}, u_{1s} = \frac{v_{on} + v_{on}}{2}, u_{1r} = \frac{v_{on} + 0}{2},$$

$$u_{2l} = \frac{0 + v_{on}}{D_t}, 0 = \frac{-v_{on} + v_{on}}{D_t}, u_{2r} = \frac{-v_{on} + 0}{D_t}.$$

In this case, the turning radius is restricted to constant value, $\rho = D_t$.

2.2 Condition for Harvesting

In this study, we focus on fields in which lettuce is planted in a row. The diagram of the vehicle and lettuce in the fields is shown in Fig. 3, where L_r is the length of a ridge, and l_c and b_c are the length and width of the imaging range of the camera installed in the front of the vehicle, respectively. P_j indicates the position of lettuce detected by a camera. The coordinates $\mathrm{P}_h(x_h, y_h)$ denote the coordinates of the top of the harvest unit and are given by

$$x_h = x - D_h\sin\theta, \tag{10}$$

$$y_h = y + D_h\cos\theta. \tag{11}$$

In this study, it is assumed that the position of lettuce from the vehicle can be obtained by the camera. The purpose of this study is to propose a control method to drive the vehicle along a row of lettuce and harvest it.

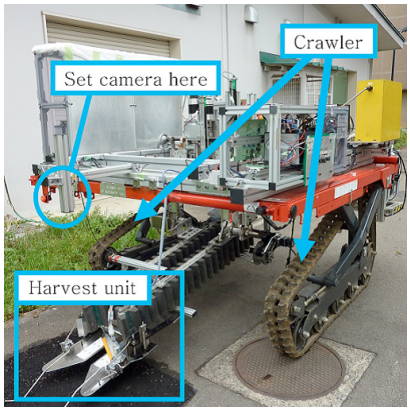

Fig. 1. Lettuce harvester

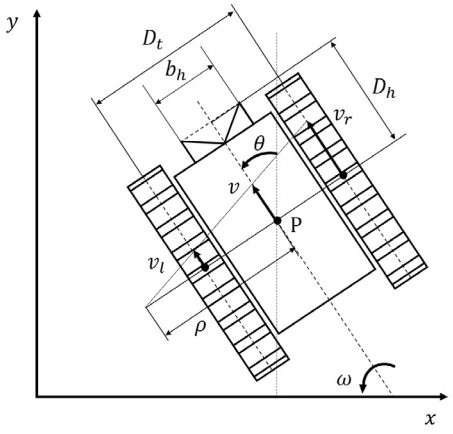

Fig. 2. Vehicle model

3. MODEL PREDICTIVE CONTROL

3.1 Outline of Model Predictive Control

In this study, MPC is used as the control method for the vehicle. In MPC, path-following control can be executed considering restriction such as the fixed turning radius of the vehicle implicitly. For a horizon T, time τ over the horizon, and number of partitions N_τ of the horizon, the sampling period of MPC is given by $\Delta\tau = T/N_\tau$, and the time step over the horizon is defined as $k(= 0, 1, 2, ..., N_\tau)$. Here, for each discrete time step $i(= 0, 1, 2, ...)$ in real time, a reference trajectory and an optimal input sequence are determined in MPC. However, it is difficult to determine

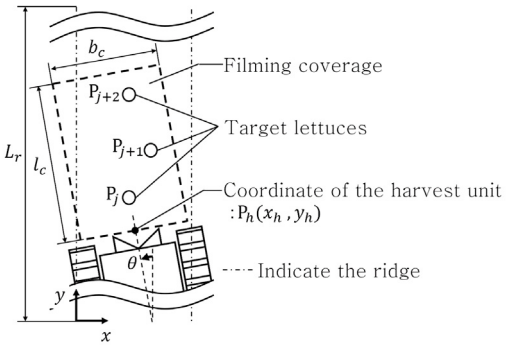

Fig. 3. Model showing filming coverage of the vehicle

an optimal input sequence for the reference trajectory because the kinematics model of (7) is a non-linear system. In addition, it is not appropriate to make the center of the vehicle follow the reference trajectory, because the harvest unit must follow a row of lettuce in order to harvest them. Therefore, in subsection 3.2, we derive a vehicle model instead of the kinematics model (7) to facilitate the application of an optimal method for determining an optimal input sequence. In subsection 3.3, we give the coordinates of the lettuce as a set-point trajectory and derive the reference trajectory to make the harvest unit follow a row of lettuce.

3.2 Vehicle Model for MPC

Since the kinematics model of (7) is a non-linear system, and inputs u_1 and u_2 are dependent on the same variables, it is difficult to determine an optimal input sequence in MPC. Therefore, the kinematics model is transformed as follows.

First, the state variables are transformed into

$$z_1(z_3) = x(t), \tag{12}$$

$$z_2(z_3) = \tan\theta(t), \quad (-\frac{\pi}{2} < \theta < \frac{\pi}{2}), \tag{13}$$

$$z_3(t) = y(t). \tag{14}$$

Next, control inputs μ_1 and μ_2 are defined as

$$\mu_1 = \frac{dz_3}{dt}(t) = v(t)\cos\theta(t) \ \ (= \text{const.}), \tag{15}$$

$$\mu_2(z_3) = \frac{\dfrac{dz_2}{dt}(t)}{\dfrac{dz_3}{dt}(t)} \ \left(\ = \frac{\omega(t)}{v(t)\cos^3\theta(t)} \right). \tag{16}$$

From these transformations, (7) is rewritten as

$$\frac{dz_3}{dt}(t) = \mu_1, \tag{17}$$

$$\frac{d}{dz_3}\begin{bmatrix} z_1(z_3) \\ z_2(z_3) \end{bmatrix} = \begin{bmatrix} 0 & -1 \\ 0 & 0 \end{bmatrix}\begin{bmatrix} z_1(z_3) \\ z_2(z_3) \end{bmatrix} + \begin{bmatrix} 0 \\ 1 \end{bmatrix}\mu_2(z_3), \tag{18}$$

where the system of Eqs. (17)-(18) is a single input system and is called the time-state control form (Sampei (1994); Sampei et al. (1996)). Here, combinations of (ω, v) are three cases from (9); therefore, μ_2 of (16) is given by three values dependent on $\theta(t)$. However, to apply a method for determining the optimal input sequences, it is desirable that μ_2 is independent of $\theta(t)$. Accordingly, in (16), $\cos\theta$ is approximated as $\cos\theta \approx 1$. In this case, $\mu_1 = v(t)$ by (16). The condition that $\mu_1 = $ const. is not satisfied in all situations in the present paper; however, it is assumed that the condition is approximately satisfied. Then, the input of the time-state control form is defined as μ_2^* given by

$$\mu_2(z_3) \approx \mu_2^*(z_3) := \frac{\omega(t)}{v(t)} \tag{19}$$

From (19), μ_2^* is given by

$$\mu_2^* \in \{\mu_{2l}^*, 0, \mu_{2r}^*\}, \tag{20}$$

$$\mu_{2l}^* = \frac{u_{2l}}{u_{1l}}, 0 = \frac{0}{u_{1s}}, \mu_{2r}^* = \frac{u_{2r}}{u_{1l}}.$$

Appendix A shows the controllability of the system using this approximation.

Table 1 shows relationships of the discrete inputs in each model.

Table 1. Input correspondence table

Velocity of track	(v_l, v_r)	$(0, v_{on})$	(v_{on}, v_{on})	$(v_{on}, 0)$
Original model	$u_1(v)$	$u_{1l}(\frac{v_{on}}{2})$	$u_{1s}(v_{on})$	$u_{1r}(\frac{v_{on}}{2})$
	$u_2(\omega)$	$u_{2l}(\frac{v_{on}}{D_t})$	$0(\frac{0}{D_t})$	$u_{2r}(-\frac{v_{on}}{D_t})$
Time-state control form	μ_1	const.		
	μ_2^*	μ_{2l}^*	0	μ_{2r}^*

Finally, the system expressed in Eqs. (17)-(18) is discretized by the zero-order hold. The sampling period is defined as $\Delta\tau$. Then, Δz_3 is given by

$$\Delta z_3 := \boldsymbol{z}_3[k+1] - \boldsymbol{z}_3[k] = \mu_1\Delta\tau. \tag{21}$$

From this, the discretized model is obtained as follows:

$$\boldsymbol{z}_{12}[k+1] = \boldsymbol{A}\boldsymbol{z}_{12}[k] + \boldsymbol{b}\mu_2^*[k], \tag{22}$$

$$\boldsymbol{z}_{12} := \begin{bmatrix} z_1 \\ z_2 \end{bmatrix}, \boldsymbol{A} := \begin{bmatrix} 1 & -\Delta z_3 \\ 0 & 1 \end{bmatrix}, \boldsymbol{b} := \begin{bmatrix} -\frac{1}{2}\Delta z_3^2 \\ \Delta z_3 \end{bmatrix}.$$

3.3 Reference Trajectory

The purpose of this study is to control the vehicle along the rows of lettuce and to harvest the produce. The reference trajectory of the top of the harvest unit is determined, and then, the trajectory of the center of the vehicle is calculated by Eqs. (10)-(11). The reference trajectory of the top of the harvest unit is defined as $\boldsymbol{Z}_h{}^{ref} = (z_{1h}^{ref}, z_{2h}^{ref}, z_{3h}^{ref})$ and is shown in Fig. 4. Here, the velocity of the reference trajectory in the z_3 $(= y)$ direction is given as a constant value, because the vehicle model is defined by the time-state control form. Then, the state variable $x_h[i]$, $y_h[i]$ and $\theta_h[i]$ of the top of the harvest unit in each sampling time in real time is regarded as the initial point. Then, the z_3 element of the reference trajectory is obtained by

$$z_{3h}^{ref}[k] = y_h[i] + k\Delta\tau\mu_1, \quad (k = 0, 1, 2, ..., N_\tau). \tag{23}$$

The final value z_{3h}^{ref} of the reference trajectory is automatically determined from (23), and the corresponding $z_1(= x)$ element is defined as the z_1 element of the coordinate of the last lettuce included in the imaging range of the camera. Thus, the reference trajectory is given by the function $z_{1h}^{ref} = S^{ref}(z_{3h}^{ref})$ connecting the initial point, coordinates of the lettuce included in the imaging range of the camera, and the final point by linear functions. For

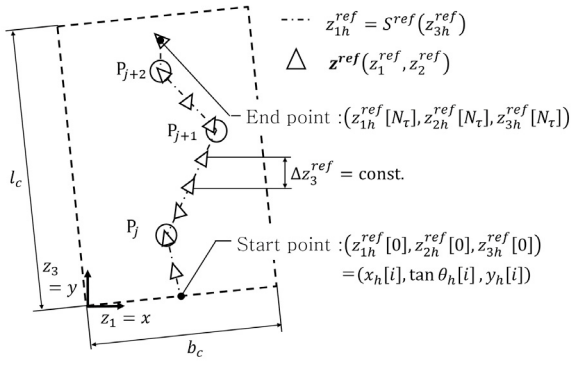

Fig. 4. Reference trajectory model

example, the reference trajectory from the initial point to the first lettuce is as follows:

$$S_1^{ref}(z_{3h}^{ref}) = \frac{x_j - x[0]}{y_j - y[0]}(z_{3h}^{ref} - y[0]) + x[0], (y[0] \le z_{3h} \le y_j). \tag{24}$$

Where (x_j, y_j) denotes coordinate of P_j. The reference trajectory S^{ref} is constructed by repeating the procedure similar to (24) until the final point. The z_1 element of the reference trajectory $(z_{1h}^{ref}[k])$ is given by

$$z_{1h}^{ref}[k] = S^{ref}(z_{3h}^{ref}[k]). \tag{25}$$

The $z_{2h}(= \tan\theta)$ element of the reference trajectory is defined by the slope of the linear function in each interval. However, to prevent steep changes of the reference angle around the lettuce, the first reference angle in each interval is given as that of the previous interval. From Eqs. (10)-(11), the reference trajectory for the center of the vehicle, $z_i^{ref}[k](i = 1, 2, 3)$, is given as follows:

$$z_1^{ref}[k] = z_{1h}^{ref}[k] + D_h \sin(\arctan z_{2h}^{ref}[k]), \tag{26}$$
$$z_2^{ref}[k] = z_{2h}^{ref}[k], \tag{27}$$
$$z_3^{ref} = z_{3h}^{ref}[k] - D_h \cos(\arctan z_{2h}^{ref}[k]). \tag{28}$$

Hereafter, the reference trajectory is used as $\boldsymbol{z_{12}^{ref}} = (z_1^{ref},\ z_2^{ref})^T$, because the error in the z_3 direction between the reference and predictive trajectories is zero.

3.4 Input Decision

In this section, the optimal input u_1^{opt}, u_2^{opt} for tracking the vehicle along the reference trajectory is derived. An input sequence in each discrete time step $k(= 0, 1, 2, ..., N_\tau)$ is defined as

$$\boldsymbol{\mu} = [\mu_2[0] \quad \mu_2[1] \quad ... \quad \mu_2[N_\tau - 1]]^{\mathrm{T}}. \tag{29}$$

Then, $\boldsymbol{\mu^{opt}}$ is defined as the input sequence minimizing the error between the predictive trajectory (the trajectory of (22) driven by the input sequence (29)) and the reference trajectory $\boldsymbol{z_{12}^{ref}} = (z_1^{ref},\ z_2^{ref})^T$. The weighted square sum of the error is given by

$$J = \frac{1}{2}(\boldsymbol{z}_{12}[N_\tau] - \boldsymbol{z}_{12}{}^{ref}[N_\tau])^{\mathrm{T}} \boldsymbol{S_f} (\boldsymbol{z}_{12}[N_\tau] - \boldsymbol{z}_{12}{}^{ref}[N_\tau]) + \frac{1}{2}\sum_{k=1}^{N_\tau - 1} (\boldsymbol{z}_{12}[k] - \boldsymbol{z}_{12}{}^{ref}[k])^{\mathrm{T}} \boldsymbol{Q} (\boldsymbol{z}_{12}[k] - \boldsymbol{z}_{12}{}^{ref}[k]), \tag{30}$$

where the positive definite matrices $\boldsymbol{Q}$ and $\boldsymbol{S_f}$ are the weight of the stage cost and that of the terminal cost, respectively (Garcia et al. (1995)). The state variable $\boldsymbol{z}_{12}[k]$ is expressed by the initial position $\boldsymbol{z}_{12}[0]$ and the input $\mu_2[k]$, and then, the cost function without the constant term (30) is defined as

$$J_\mu = \left\{ \boldsymbol{z}_{12}[0]^{\mathrm{T}} (\boldsymbol{A}^{N_\tau})^{\mathrm{T}} - \boldsymbol{z}_{12}{}^{ref}[N_\tau]^{\mathrm{T}} + \frac{1}{2}\boldsymbol{\mu}^{\mathrm{T}} \boldsymbol{H}_{N_\tau}^{\mathrm{T}} \right\} \boldsymbol{S_f} \boldsymbol{H}_{N_\tau} \boldsymbol{\mu} + \sum_{k=1}^{N_\tau - 1} \left\{ \boldsymbol{z}_{12}[0]^{\mathrm{T}} (\boldsymbol{A}^k)^{\mathrm{T}} - \boldsymbol{z}_{12}{}^{ref}[k]^{\mathrm{T}} + \frac{1}{2}\boldsymbol{\mu}^{\mathrm{T}} \boldsymbol{H}_k^{\mathrm{T}} \right\} \boldsymbol{Q} \boldsymbol{H}_k \boldsymbol{\mu}, \tag{31}$$

where

$$\boldsymbol{H}_k = [\boldsymbol{A}^{k-1}\boldsymbol{b} \quad \boldsymbol{A}^{k-2}\boldsymbol{b} \quad ... \quad \boldsymbol{b} \quad \boldsymbol{0}_{2\times(N_\tau - k)}].$$

The optimal input sequence $\boldsymbol{\mu^{opt}}$ is obtained by minimizing J_μ, because J_μ denotes the magnitude of the error between the reference and predictive trajectories. Since $\boldsymbol{Q}$ and $\boldsymbol{S_f}$ are positive definite, J_μ is a convex quadratic form function. Then, the neighborhood input sequence $\boldsymbol{\mu^{opt}}$ of the optimal input can be calculated using the gradient vector of J_μ. In this study, to solve the optimal problem in real time, the optimal method based on gradient methods (Maruyama et al. (2013)) is adopted. The control inputs u_1^{opt} and u_2^{opt} are calculated by the first element $\mu_2^{opt}[0]$ of the obtained input sequence $\boldsymbol{\mu^{opt}}$ from Table 1. Hereafter, the proposed method serves as the control method of this procedure.

4. NUMERICAL SIMULATION

4.1 Simulation Conditions

Numerical simulations are performed by a general-purpose PC with an Intel core i7-4770 CPU with 3.4 GHz and 8 GB RAM.

The reference trajectory is determined for 10 heads of lettuce as shown in Fig. 5(a), and the length of the ridge is $L_r = 3.0$ m. The other parameters are as follows: the acquisition period for the coordinates of the lettuce is $\Delta t = 40$ ms, the horizon is $T = 13.0$ s, the number of partitions is $N_\tau = 13$, the velocity of the crawler is $v_{on} = 0.060$ m/s, and the initial position of the center of the vehicle is $\boldsymbol{x}[0] = [0.300\text{ m},\ -1.350\text{ m},\ 0.0\text{ rad}]^{\mathrm{T}}$. Accordingly, the sampling period and velocity in the z_3 direction are derived as $\Delta\tau = 1.00$ m/s and $\mu_1 = 0.060$ m/s, respectively. The parameters of the vehicle are shown in Table 2. Since u_1 and u_2 are defined by (9), μ_2^* is defined as

$$\mu_2^* \in \begin{cases} \mu_{2l}^* \approx \ \ 1.481, \\ \mu_{20}^* = \ \ 0, \\ \mu_{2r}^* \approx -1.481. \end{cases} \tag{32}$$

We specified the weighting matrices as

$$\boldsymbol{S_f} = \mathrm{diag}(s_{f1},\ s_{f2}) = \mathrm{diag}(1,\ 0.1), \tag{33}$$
$$\boldsymbol{Q} = \mathrm{diag}(q_1,\ q_2) = \mathrm{diag}(15,\ 10). \tag{34}$$

4.2 Comparison Approach

In this study, comparison approaches are defined as methods driving the vehicle to the nearest lettuce. Specifically, in the comparison approaches, the x-coordinate of the top

Table 2. Vehicle parameters

D_t	Centre of left track to center of right track	1.350 m
D_h	Vehicle center to top of harvesting mechanism	0.930 m
b_h	Width of harvest unit	0.050 m
l_c	Length of filming coverage	0.420 m
b_c	Width of filming coverage	0.300 m

of the harvest unit is set to that of the nearest lettuce based on the on-off control theory. The following two switching laws are used:

Comparison approach 1:

$$\begin{aligned}
&\text{if} \quad x_h < x_j \\
&\qquad \text{turn right } ((\mathrm{u}_1, \mathrm{u}_2) = (\mathrm{u}_{1\mathrm{r}}, \mathrm{u}_{2\mathrm{r}})) \\
&\text{elseif} \quad x_h > x_j \\
&\qquad \text{turn left } ((\mathrm{u}_1, \mathrm{u}_2) = (\mathrm{u}_{1\mathrm{l}}, \mathrm{u}_{2\mathrm{l}})) \\
&\text{else} \\
&\qquad \text{go straight } ((\mathrm{u}_1, \mathrm{u}_2) = (\mathrm{u}_{1\mathrm{s}}, 0)) \\
&\text{end}
\end{aligned}$$

Comparison approach 2:

$$\begin{aligned}
&\text{if} \quad x_h + \frac{b_h}{2} < x_j \\
&\qquad \text{turn right } ((\mathrm{u}_1, \mathrm{u}_2) = (\mathrm{u}_{1\mathrm{r}}, \mathrm{u}_{2\mathrm{r}})) \\
&\text{elseif} \quad x_h - \frac{b_h}{2} > x_j \\
&\qquad \text{turn left } ((\mathrm{u}_1, \mathrm{u}_2) = (\mathrm{u}_{1\mathrm{l}}, \mathrm{u}_{2\mathrm{l}})) \\
&\text{else} \\
&\qquad \text{go straight } ((\mathrm{u}_1, \mathrm{u}_2) = (\mathrm{u}_{1\mathrm{s}}, 0)) \\
&\text{end}
\end{aligned}$$

Comparison approach 1 switches the input according to the position of the top of the harvest unit (i.e., whether it is present on the left- or right-hand side of the reference trajectory). If the top of the harvest unit is aligned with the reference trajectory, the vehicle runs straight. Comparison approach 2 provides a margin of the harvest unit width, b_h, as a switching criterion. If the alignment of the top of the harvest unit exceeds the margin, the input is switched based on the rule in comparison approach 1.

4.3 Results and Discussion

Figs. 5(b)-(d) show trajectories of the top of the harvest unit in the proposed method, comparison approach 1, and comparison approach 2, respectively. Figs. 6-8 show histograms of the proposed method, comparison approach 1, and comparison approach 2, respectively, where d_{lc} denotes the distance between the center of the harvest unit and each lettuce, and the histogram bin is 0.005 m. Table 3 shows the number of input switching, μ_{swi}, until the end of the simulation. From Figs. 5-8, the application of the proposed method and comparison approach 1 allows tracking of the lettuce.

In contrast, the tracking performance of comparison approach 2 shows that it cannot harvest lettuce at the center of the harvest unit because the margin for the harvest unit width was given to the switching criterion. The stalk diameter of lettuce is approximately 30 mm. Therefore, the proposed method and comparison approach 1 are practical methods compared with comparison approach 2. From Table 3, the number of switchings of the proposed method

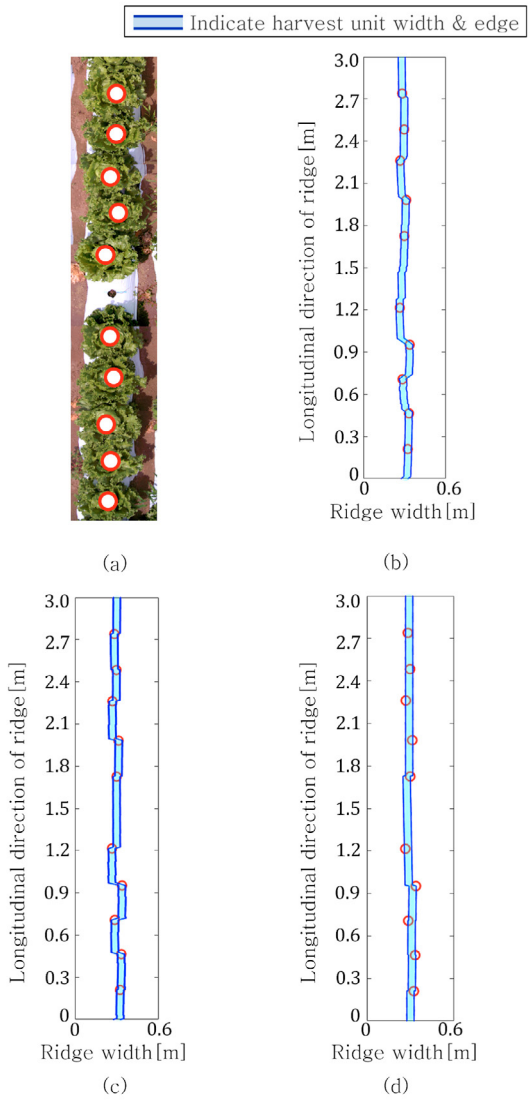

Fig. 5. Harvest unit trajectory

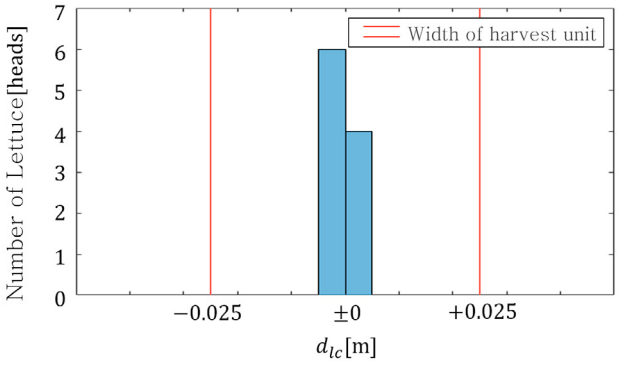

Fig. 6. Histogram of proposed method

and comparison approach 2 are one-thirty and one three-hundredths compared with that of comparison approach 1. The increase in the number of switchings causes the vehicle to swing and mechanical stress. From the viewpoint of the number of switchings, the proposed method and

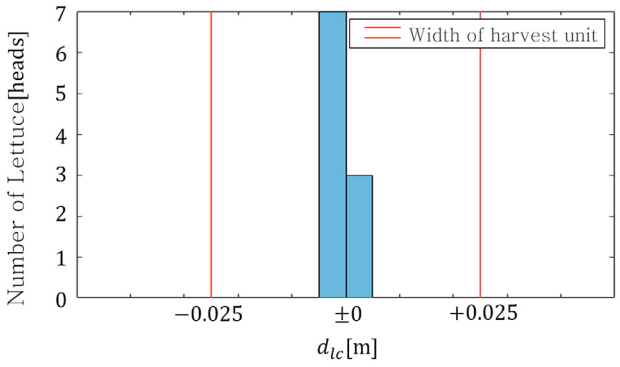

Fig. 7. Histogram of comparative approach 1

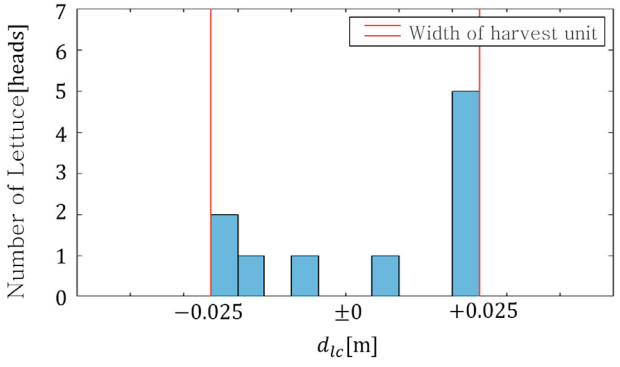

Fig. 8. Histogram of comparative approach 2

Table 3. Number of times switching was needed

	μ_{swi}[times]
Proposed method	117
comparative approach 1	3185
comparative approach 2	10

comparison approach 2 are useful. In the proposed method, the average time T_{ave} of calculation for solving the optimal problem is 3.6 ms, which is sufficient small compared to the sampling period of 40 ms. Thus, the proposed method provides sufficient accuracy in terms of harvesting motion while suppressing the number of switchings. Furthermore, the motion can be carried out in real time.

5. CONCLUSION

In this paper, we proposed a control method for a lettuce harvester with on-off actuators based on the relative positions of the lettuce and the harvester. We proved that the optimal neighborhood discrete input can be obtained by deriving the time-state control form and utilizing MPC. The simulation results showed the effectiveness of the proposed method. Thus, the proposed method drastically reduces the chances of damage to farm produce not grown in straight rows, unlike robots using only a map with a GPS.

REFERENCES

Iida, M., Uchida, R., Zhu, H., Suguri, M., Kurita, H., and Masuda, R. (2013). Path-following control of a head-feeding combine robot. Engineering in Agriculture, Environment and Food, 6(2), pp. 61-67.

Noguchi, N., Will, J., Reid, J., and Zhang, Q. (2004). Development of a master-slave robot system for farm operations. Computers and Electronics in Agriculture, 44, pp. 1-19.

O'Connor, M., Bell, T., Elkaim, G., and Parkison, B. (1996). Automatic steering of farm vehicles using GPS. Proc. 3rd Int. Conf. Precision Farming, pp. 767-777.

Kise, M., Zhang, Q., and Mas, Rovira, F. (2005). A stereovision-based crop row detection method for tractor-automated guidance. Biosystems Engineering, 90(4), pp.357-367.

Keicher, R., and Seufert, H. (2000). Automatic guidance for agricultural vehicles in Europe. Cinoyters and Electronics in Agriculture, 25(1/2), pp.169-194.

Fukao, T., Nakagawa, H., and Adachi, N. (2000). Adaptive tracking control of a nonholonomic mobile robot. IEEE Trans. Robot. Autom., vol. 16, no. 5, pp. 609-615

Nagasaka, Y., Umeda, N., Kanetai, Y., Taniwaki, K., and Sasaki, Y. (2004). Autonomous guidance for rice transplanting using global positioning and gyroscopes. Computers and Electronics in Agriculture, 43(3), pp.223-234.

Ahmadi, M., Polotski, V., and Hurteau, R. (2000) Path tracking control of tracked vehicles. Proc. IEEEE Int. Conf. on Robotics and Automation, pp.2938-2943.

Maruyama, N., Chida, Y., and Ikeda, Y. (2013). Model predictive control of pneumatic isolation table with quantized input. Proc. SICE Annual Conference, pp. 727-732.

Sampei, M. (1994). A control strategy for a class of non-holonomic systems-time state control form and its application. Proc. 33rd CDC, pp. 1120-1121.

Sampei, M., Kiyota, H., Koga, M., and Suzuki, M. (1996). Necessary and sufficient conditions for transformation of nonholonomic system into time-state control form. Proc. 35th CDC, pp. 4745-4746.

William, S., Levine (1995). The control handbook. CRC press.

Garcia, C.E., Prett, D.M., and Morari, M. (1989). Model predictive control:Theory and practice-a survey. Automatica, 25(3), pp. 335-348.

Appendix A. CONTROLLABILITY OF THE SYSTEM AFTER APPROXIMATION

When approximating $\mu_1 = v(t)$ and $\mu_2 = \frac{\omega(t)}{v(t)}$, the approximated kinematics model is given by

$$\dot{\boldsymbol{x}}(t) = \boldsymbol{f_1}^*(\boldsymbol{x}(t))u_1(t) + \boldsymbol{f_2}^*(\boldsymbol{x}(t))u_2(t), \tag{A.1}$$

$$\boldsymbol{x}(t) := \begin{bmatrix} x(t) \\ y(t) \\ \theta(t) \end{bmatrix},$$

$$\boldsymbol{f_1}^*(\boldsymbol{x}(t)) := \begin{bmatrix} -\theta(t) \\ 1 \\ 0 \end{bmatrix}, \ \boldsymbol{f_2}^*(\boldsymbol{x}(t)) := \begin{bmatrix} 0 \\ 0 \\ 1 \end{bmatrix}.$$

From (7) and (A.1), $\boldsymbol{f_2}$ includes an error in the approximated kinematics model. The Lie bracket of (A.1) is obtained by

$$[\boldsymbol{f_1}^*, \boldsymbol{f_2}^*](\boldsymbol{x}) = \frac{\partial \boldsymbol{f_2}^*}{\partial \boldsymbol{x}} \boldsymbol{f_1}^*(\boldsymbol{x}) - \frac{\partial \boldsymbol{f_1}^*}{\partial \boldsymbol{x}} \boldsymbol{f_2}^*(\boldsymbol{x}) = \begin{bmatrix} 1 \\ 0 \\ 0 \end{bmatrix}. \tag{A.2}$$

The three-dimensional space is spanned by (A.2), $\boldsymbol{f_1}^*(\boldsymbol{x})$, and $\boldsymbol{f_2}^*(\boldsymbol{x})$. Accordingly, the system is globally controllable; but, from (13), the motion of the time-state control form is restricted in $(-\frac{\pi}{2} < \theta < \frac{\pi}{2})$. However, the transformations of Eqs. (12)-(14) and (19) can be applied because the vehicle follows a straight row of lettuce in this study.